Acta Crystallographica Section B
Structural Science
ISSN 0108-7681

Modulated crystal structure of incommensurate low tridymite

Heribert A. Graetsch

Institut für Geologie, Mineralogie and Geophysik, Ruhr-Universität Bochum, Bochum D44780, Germany

Correspondence e-mail: heribert.graetsch@rub.de

Received 27 January 2009
Accepted 22 July 2009

The incommensurately modulated crystal structure of low SiO_2 tridymite was refined based on single-crystal X-ray diffraction data in the superspace group $Cc(\alpha 0 \gamma)0$. The data set consists of 885 main reflections, 1751 first-order, 924 second-order and 119 third-order satellite reflections with $I > 3\sigma(I)$. The modulation is mainly made up from cooperative twistings of the rigid SiO_4 tetrahedra. Two orders of displacement waves are used to describe the modulation of the Si atoms and three orders for the O atoms. The maximal amplitudes are *ca* 0.6 Å. O atoms bridging pairs of tetrahedra in *cis* and *trans* configurations show different positional modulation patterns. The anisotropic displacement parameters (ADPs) are also modulated. A correlation between ADP modulations and positional modulations was found.

1. Introduction

Tridymite has a displacively flexible framework of corner-sharing tetrahedra (Withers *et al.*, 2004). Rotations and tilting of the rigid tetrahedra with respect to each other result in various different relative orientations of neighbouring tetrahedra. Apart from several modifications that exist at high temperatures, three differently distorted low-temperature forms of silica tridymite can be distinguished at ambient temperatures (Table 1). One of these room-temperature modifications is incommensurately modulated. The modulation vector and the lattice parameters were refined from X-ray powder diffraction data as $\mathbf{r} = 0.6632\ (14)\mathbf{a}^* - 0.4980\ (6)\mathbf{c}^*$ with respect to a pseudo-orthohexagonal setting of the average structure in the space group *Cc* [a= 5.0079 (2), b = 8.6004 (4), c = 8.2169 (5) Å and $\beta = 91.512\ (5)^\circ$; Hoffmann *et al.*, 1983]. The wavevector depends only slightly on the temperature (Graetsch & Brunelli, 2005). Incommensurate low tridymite has been referred to in the literature as MX-1 (Nukui & Nakazawa, 1980; M: monoclinic), S1 (Sato, 1964; S: stable), L3-T_O (Löns & Hoffmann, 1987; L: low, T: tridymite, O: ordered) and L3-T_O(MX-1) (Graetsch & Topalović-Dierdorf, 1996).

In tridymite, layers with six-membered rings of tetrahedra are stacked in an antiparallel orientation to give a two-layer sequence. Viewed along the hexagonal c axis, the layers are positioned in a totally eclipsed position in the hexagonal high-temperature modifications, leaving open channels in the structure. Upon cooling, tridymite undergoes a cascade of displacive phase transitions (Table 1). Different rigid unit modes successively freeze in by way of forming phases with collapsed rings of tetrahedra (Pryde & Dove, 1998). In a first step, alternate layers of tetrahedra are laterally shifted with respect to each other below 653 K, reducing the symmetry to orthorhombic (Graetsch, 2001). In a second step, an incom-

Table 1
Space-group symmetries and temperature ranges of SiO_2 tridymite.

	SiO_2	Temperature (K)	Remarks
H1-T(HP)†	$P6_3/mmc$‡	653–1723	Dynamically disordered
H2-T(OC)†	$C222_1$§	473–723	Dynamically disordered
H3-T(OS)†	$P2_1(\alpha\beta 0)$¶	423–473	Incommensurately modulated and dynamically disordered
H4-T(OP)†	$P2_12_12_1$††	383–423	Commensurately modulated
L1-T_O(MC)†	Cc‡‡	< 383	Commensurately modulated
L2-T_D(PO5/10)†	$F1$§§		Commensurately modulated
L3-T_O(MX-1)†	$Cc(\alpha 0\gamma)$¶¶		Incommensurately modulated

† Nomenclature according to Löns & Hoffmann (1987), Flörke & Nukui (1988) and Nukui *et al.* (1978) (in brackets). ‡ Gibbs (1927); an additional hexagonal–hexagonal transition near 723 K was reported by DeDombal & Carpenter (1993) and Cellai *et al.* (1994). § Dollase (1967) and Kihara *et al.* (1986). ¶ Nukui *et al.* (1979) and Graetsch & Brunelli (2005). †† Nukui *et al.* (1978) and Kihara (1977). ‡‡ Dollase & Baur (1976), Kato & Nukui (1976), Baur (1977) and Kato *et al.* (1998). §§ Konnert & Appleman (1978). ¶¶ Löns & Hoffmann (1987), Graetsch & Topalović-Dierdorf (1996), Graetsch (2003) and this work. L3-T_O(MX-1) undergoes an additional phase transformation near 338 K (Hoffmann *et al.*, 1983).

mensurately modulated phase with a strongly temperature-dependent wavevector is formed at about 493 K (Nukui *et al.*, 1979; Graetsch & Brunelli, 2005) which discontinuously locks in at *ca* 423 K resulting in a superstructure with tripled *a* lattice parameter (Kihara, 1977; Graetsch, 2001). Finally, a monoclinic phase [L1-T_O(MC)] with a complex superstructure is formed at 389 K in a first-order transformation (Kato & Nukui, 1976). This transformation path, however, can be modified by thermal or mechanical stress or by lattice imperfections like stacking faults. Most tridymites occurring in terrestrial rocks contain stacking faults. They have a triclinic (pseudo-orthorhombic) superlattice L2-$T_D(PO_{5/10})$ with doubled *a* and *b* lattice parameters and a tenfold *c* axis compared with the unit cell of the orthorhombic high-temperature tridymite H2-T_O(OC) (*cf.* Table 1).

L1-T_O(MC) also occurs in nature, however, in contrast to L2-T_D(PO5/10), it was more abundantly detected in meteorites and moon rocks rather than in terrestrial rocks. A natural occurrence of incommensurate low tridymite L3-T_O(MX-1) is not known. It can be obtained from L1-T_O(MC) either by annealing above 388 K and subsequent quenching to 263 K or at ambient conditions by the application of uniaxial pressure (Hoffmann *et al.*, 1983). Partial transformation of L1-T_O(MC) to L3-T_O(MX-1) can be produced by grinding, *i.e.* for powder diffraction purposes. The density of L3-T_O(MX-1) is slightly higher than those of the naturally occurring forms of tridymite. This indicates a rather incomplete collapse of the framework of corner-sharing tetrahedra in comparison to the other low-temperature modifications L1-T_O(MC) and L2-T_D(PO5/10). The lower density might also indicate a lower stability of incommensurate low tridymite.

The crystal structure of incommensurate low tridymite was determined by Löns & Hoffmann (1987) from X-ray single-crystal data in the space group *C*1. They used a commensurate $3 \times 1 \times 2$ superstructure as an approximation. All six-membered rings of $SiO_{4/2}$ tetrahedra have a ditrigonal shape in incommensurate low tridymite (Löns & Hoffmann, 1987), whereas monoclinic L1-T_O(MC) and pseudo-orthorhombic L2-T_D(PO5/10) low tridymite either contain oval and ditrigonal rings or are entirely made up of rings with an oval shape. The crystal structure has been refined based on X-ray powder diffraction data using the superspace-group formalism (Graetsch, 2003). The modulation can be described in the space group $Cc(\alpha 0\gamma)0$ as wavy shifts and tilting of the rigid tetrahedra with a maximal amplitude of *ca* 0.6 Å.

Only first-order satellite reflections were visible in the powder diagram (Graetsch, 2003). Single-crystal diffracto-

Table 2
Experimental data.

Crystal data	
Chemical formula	SiO_2
M_r	60.1
Cell setting, superspace group	Monoclinic, $Cc(\alpha 0\gamma)0$
Temperature (K)	298
a, *b*, *c* (Å)	5.0049 (12), 8.6044 (18), 8.214 (3)
β (°)	91.54 (3)
V (Å^3)	354.60 (2)
Z	8
Radiation type, wavelength (Å)	Mo $K\alpha$, 0.71069
μ (mm^{-1})	0.848
Modulation wavevector	0.6543 (7)**a*** − 0.4946 (9)**c***
Crystal form, size (mm)	Plate, *ca* 0.0001
Data collection	
Diffractometer	Xcalibur CCD
Data collection method	2φ and 4ω scans
Absorption correction	None
No. of measured, independent and observed reflections	23 131, 7927, 3679
Criterion for observed reflections	$I > 3\sigma(I)$
No. of main reflections (obs, all)	885, 1153
No. of first-order satellites (obs, all)	1751, 2301
No. of second-order satellites (obs, all)	924, 2362
No. of third-order satellites (obs, all)	119, 2211
R_{int} (obs/all)	3.38, 4.02
R_{int}(main reflections) (obs/all)	2.77, 2.87
R_{int} (all), R_{int} (obs), first-order satellites	3.65, 3.95
R_{int} (all), R_{int} (obs), second-order satellites	7.34, 10.00
R_{int} (all), R_{int} (obs), third-order satellites	14.13, 36.25
θ_{max} (95%)	32.47
Refinement	
Refinement on	F
R_{all}, wR_{all}	7.55, 3.59
R_{obs}, wR_{obs}	3.03, 2.95
R_{obs}, wR_{obs}, R_{all}, wR_{all} (main reflections)	2.36, 2.63, 3.33, 2.69
R_{obs}, wR_{obs}, R_{all}, wR_{all} (first-order satellites)	2.92, 2.85, 4.84, 3.38
R_{obs}, wR_{obs}, R_{all}, wR_{all} (second-order satellites)	4.62, 4.37, 10.80, 5.22
R_{obs}, wR_{obs}, R_{all}, wR_{all} (third-order satellites)	8.93, 10.58, 34.25, 22.68
S_{obs}, S_{all}	1.22, 0.99
No. of reflections	7927
No. of parameters	293
$(\Delta/\sigma)_{max}$	0.008
$\Delta\rho_{max}$, $\Delta\rho_{min}$ (e Å^{-3})	0.36, −0.34
Isotropic extinction correction	0.464 (10)

Computer programs used: *JANA*2006 (Petříček *et al.*, 2006), *NADA* (Schönleber *et al.*, 2001), *CrysAlisCCD* (Oxford Diffraction, 2006*a*), *CrysAlis RED* (Oxford Diffraction, 2006), *DIAMOND*3.0 (Brandenburg & Putz, 2005).

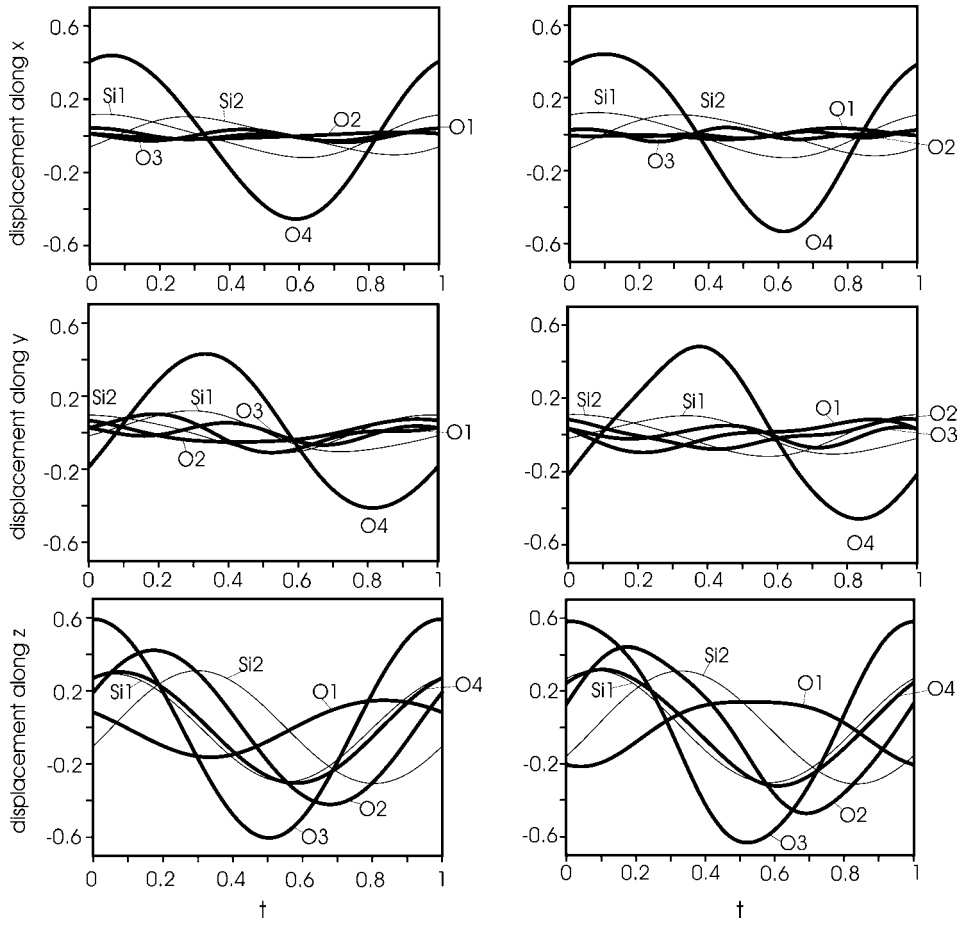

Figure 1
Deviations in Å of the atoms from their average positions *versus* the internal *t* coordinate. Left: results from powder diffraction (Graetsch, 2003); right side: results from single-crystal refinement (this work).

grams, however, showed satellites up to third order (Löns & Hoffmann, 1987; Graetsch & Topalović-Dierdorf, 1996). In the present study all satellite reflections are included in the refinement, so that the actual shape of the modulation function can be determined. The powder data only allowed a refinement of one single overall displacement parameter (Graetsch, 2003), whereas the new single-crystal data enables a refinement of individual ADPs and their modification by the displacive positional modulation.

2. Experimental

Crystals of SiO_2 tridymite were grown by Flörke & Langer (1972) at 1673 K from a Na_2WO_4 flux with subsequent hydrothermal treatment at temperatures between 1088 and 1223 K and 200 bars H_2O. Most of the colourless clear crystals consist of monoclinic tridymite L1-T_O(MC), but a few very thin plates showing only very low birefringence under a polarizing microscope consisted of incommensurate low tridymite L3-T_O(MX-1). A platelet with a thickness of less than 0.01 mm and *ca* 0.10 mm lateral extension showing homogeneous extinction under crossed polars was selected and fixed on top of a glass fibre using a two-component glue (Uhu 300). The latter allows X-ray diffraction experiments at elevated temperatures.

Initially, the X-ray diffraction patterns showed pseudo-hexagonal twinning. Owing to the small deviation of the monoclinic angle of 91.5° from orthorhombic symmetry, the twinning caused partial overlap of reflections from different twin individuals. Heating to 398 K which is above the first two high-temperature phase transitions near 338 and 388 K and rapid subsequent cooling produced an untwinned crystal. The untwinning appears to be caused or influenced by stress from the thermally altered glue.

A single-crystal data set was collected on a four-circle kappa diffractometer (Xcalibur, Oxford Diffraction) equipped with a CCD detector and an enhanced X-ray source. Mo $K\alpha$ radiation was obtained from a graphite monochromator. The sample-to-detector distance was 60 mm. Two φ and four ω scans were measured at a step width of 0.5°. The exposure time was 10 s per frame. Satellite reflections up to third order were observed. However, the intensities of only a few third-order satellites exceeded 3σ (Table 2). Data reduction was carried out with the program *CrysAlisRED* (Oxford Diffraction, 2006*b*). An absorption correction was considered unnecessary.[1]

3. Refinement

The crystal structure was refined in the 3 + 1-dimensional superspace group $Cc(\alpha 0\gamma)0$ with the program *JANA*2006 (Petříček *et al.*, 2006), starting with the positional parameters obtained from X-ray powder diffraction (Graetsch, 2003).

Contrary to the previous refinement of powder data, individual atomic displacement parameters could be distinguished. Initially, the average crystal structure was refined in the space group *Cc* using main reflections exclusively. Soft restraints were applied so that the Si—O bonding distances and the tetrahedral O—Si—O angles were close to 1.60 (1) Å

[1] Supplementary data for this paper are available from the IUCr electronic archives (Reference: CK5037). Services for accessing these data are described at the back of the journal.

and 109.5 (9)°. The ADPs were largest for the O2, O3 and O4 atoms indicating strong involvement of these atoms in the modulation.

Including all satellite reflections, refinement of first- and second-order harmonic positional modulation waves for the Si atoms and first-through third-order waves for the O atoms resulted in *wR* for all reflections of 0.0436. The *R* values for the third-order satellites remained rather high presumably due to their feeble intensity. The restraints on the Si—O bonding distances were removed in the final cycles of the refinement, and replaced by softer restraints so that the lengths of the four bonds were allowed to refine to a common value for each of the two symmetrically independent tetrahedra, but were not allowed to be varied in the course of the displacive modulation. Additional refinement of first- and second-order modulations of the ADPs reduced the *wR*(all) value further to 0.0359 (*cf.* Table 2). Refinement of even higher-order harmonics yielded only a very small additional reduction of the *R* values and was considered insignificant. The remaining difference electron density did not exceed ± 0.36 e.

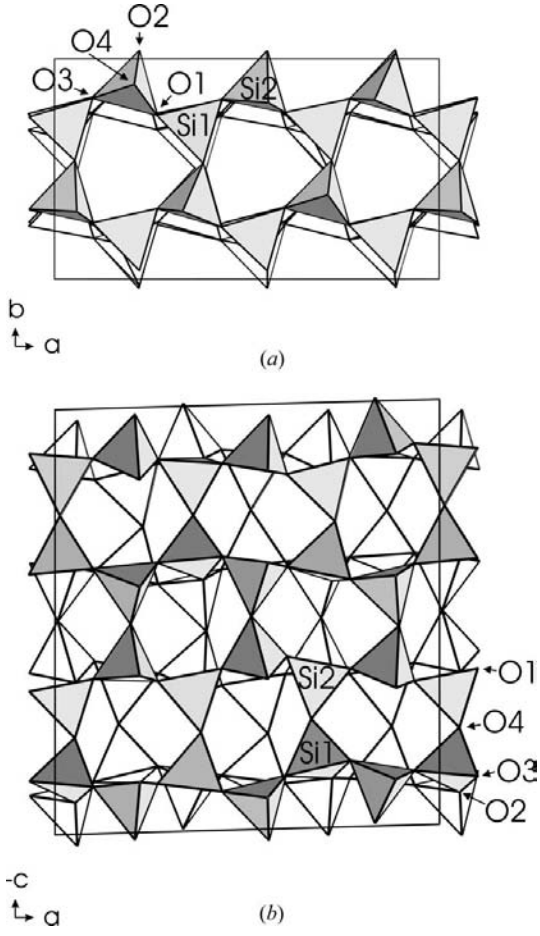

Figure 2
Tetrahedral representation of incommensurately modulated low tridymite. The cell edges refer to a 3 × 1 × 2 commensurate approximation to the incommensurate superstructure. (*a*) View along the pseudo-hexagonal *c* axis at ditrigonal six-membered rings of tetrahedra with alternating tetrahedra pointing up and down. (*b*) View along the *b* axis at six-membered rings of tetrahedra with pairs of tetrahedra pointing to the same direction (*cis* configuration). The displacive modulation consists of a combination of wavy shifts and tilting of the tetrahedra.

4. Discussion

Contrary to the orthorhombic and hexagonal high-temperature modifications existing above *ca* 493 and 653 K, the two Si atoms are no longer symmetrically equivalent in incommensurate low tridymite. The amplitudes of the displacive modulations, however, are virtually the same for Si1 and Si2 (Fig. 1), but the phase is shifted. Displacements along the *c* axis are larger (*ca* 0.3 Å) than in the perpendicular direction (*ca* 0.1 Å). The shapes of the modulation functions obtained from powder and single-crystal data differ only very slightly.

Conversely, the modulation of the O atoms shows some striking differences. O4 has large displacement amplitudes of more than 0.4 Å along *x* and *y*, whereas the modulations of O1, O2 and O3 are even smaller than those of the Si atoms in these directions. O3 displays the largest amplitude, *i.e. ca* 0.6 Å along *z*. The modulation of O2 is also larger than that of O4 in this direction, while the amplitude is smallest for O1 (Fig. 1).

The O atoms are not symmetrically equivalent in hexagonal high tridymite. O4 links two tetrahedra in such a way that the pair of tetrahedra is in a *cis* configuration. O1, O2 and O3 are bridging tetrahedra that are in a *trans* configuration (Fig. 2). The *cis* configuration has been considered energetically less favourable than the *trans* configuration, since the O atoms have larger interatomic distances and better shielding in the *trans* configuration (Flörke, 1967).

In incommensurate low tridymite, O atoms in different configurations show markedly different involvement in the modulation (O4 *versus* O1, O2 and O3). The symmetry reduction of the hexagonal–orthorhombic phase transition near 653 K makes O1 symmetrically inequivalent to O2 and O3. This also appears to be reflected in the different involvement in the positional modulation where O1 shows the

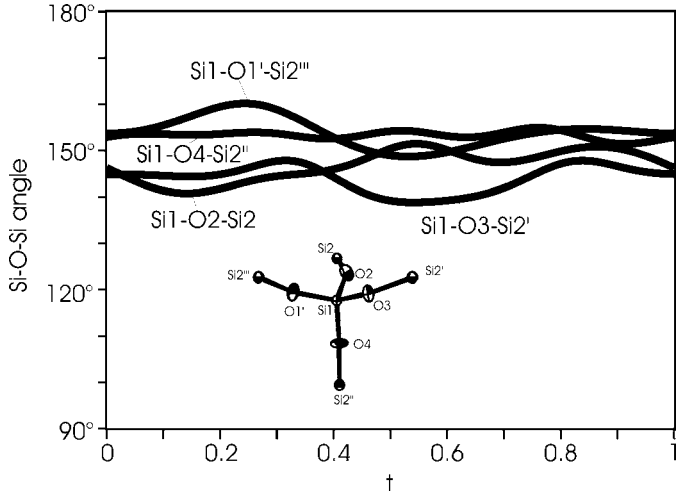

Figure 3
Variation of the intertetrahedral Si—O—Si angles with the internal *t* coordinate.

smallest displacements, and O2 and O3 have similar amplitudes (Fig. 1).

The incorporation of higher-order satellites in the single-crystal data reveals that the actual shapes of the positional modulations of the O atoms differ from the simple harmonic waves as determined by powder diffraction. The difference can most easily be seen in the displacement curve along *z* of O1 (Fig. 1).

The displacement amplitudes of the O atoms at the edges of the tetrahedra are higher than those of the Si atoms located at the centres of the tetrahedra, indicating that the modulation consists of rotations or tiltings of the rigid tetrahedra rather than shifts of whole tetrahedral units. The Si—O bonding distances and O—O tetrahedral edges are not modulated, but the Si—O—Si intertetrahedral angles and torsions of the tetrahedra vary along the modulation vector (Figs. 3 and 4). Again, differences can be observed for *cis* and *trans* configurations of tetrahedra. The modulation of the Si—O—Si angles is very weak for the O4 bridging atom at the *cis* configuration compared with *ca* $\pm 5^\circ$ for the other O atoms bridging *trans* configurations (Fig. 3). The smallest torsion angles are only *ca* $\pm 2^\circ$ around O4 and up to $\pm 25^\circ$ around O1 (Fig. 4).

The average intertetrahedral Si—O—Si angle of incommensurately modulated low tridymite is 149.5 (4.9)°, which is close to the corresponding values for monoclinic and pseudo-orthorhombic low tridymite of 149.9 (7.4) and 148.3°, but

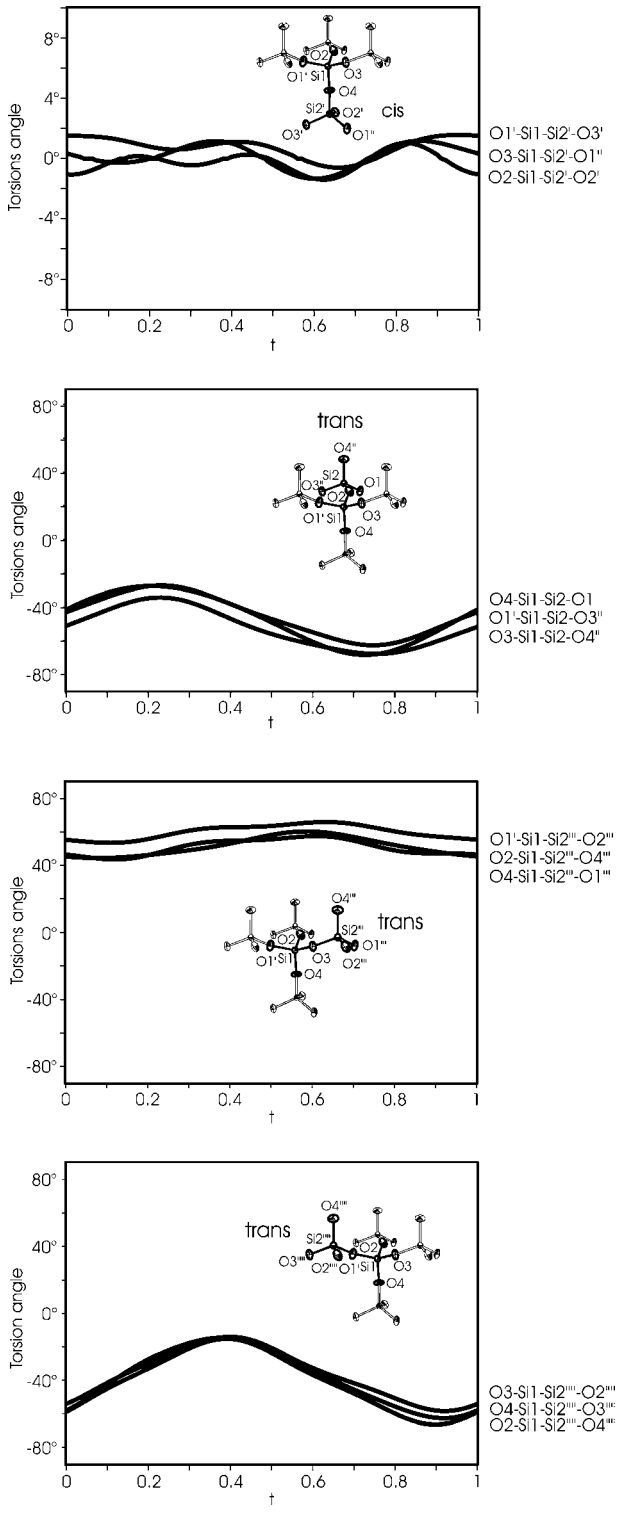

Figure 4
Variation of the torsion angles between adjacent tetrahedra along the internal *t* coordinate. The torsion was measured as O—Si···Si—O angles neglecting the bridging O atoms. Note the different scales for tetrahedra in the *cis* configuration (at the top) and in the *trans* configuration.

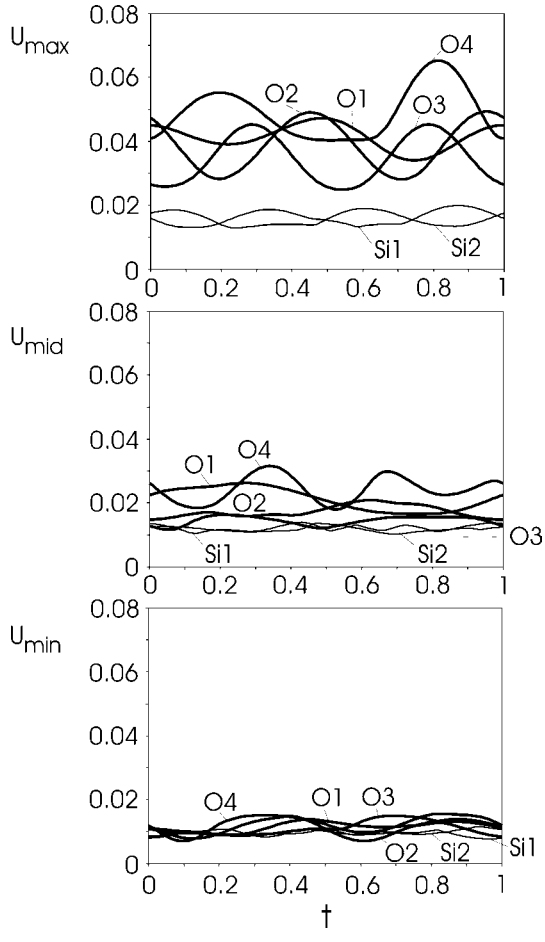

Figure 5
Anisotropic displacement parameters representing the principal axes of the U^{ij} tensors as a function of the internal *t* coordinate. The thick lines refer to O atoms and the thin lines to the Si atoms.

significantly larger than in quartz (143.5°) and cristobalite (146.8°). Very large or almost straight Si—O—Si angles as observed in the other low tridymite phases do not occur in incommensurate low tridymite. The basic structure has an apparent Si1—O4—Si2 angle of 177.2° at the *cis* configuration. However, this value is obviously mimicked by averaging over the static displacements of the atoms owing to the positional modulation. The true Si1—O4—Si2 angle is only 153.3° on average.

Owing to the varying environments of the atoms, the large amplitudes of the positional modulations are accompanied by modulations of the ADPs. As for the position modulation, the ADP modulations are stronger for the O atoms than for the Si atoms (Fig. 5). The amplitudes are largest for O4 along the *a* and *b* axes and relatively small along *c*. The modulation is strongest for O3 in the latter direction. The ADP modulation is relatively small for O1. The position modulations of the O atoms are so sharp that their four-dimensional electron-density distributions appear as slightly discontinuous, even after summing up in their 2 × 2 × 2 Å domains (Fig. 6).

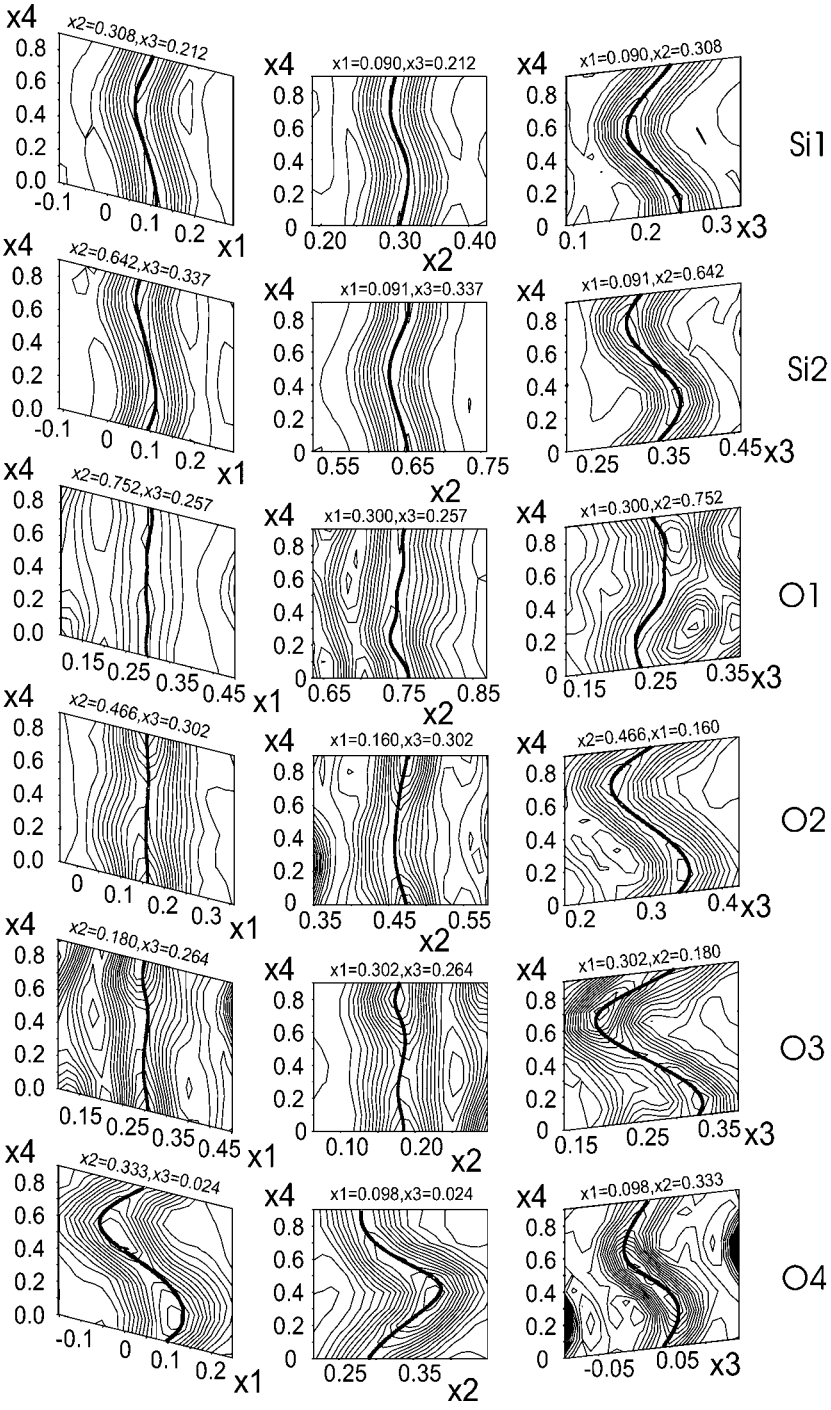

Figure 6
Sections of the Fourier maps (obs) in superspace (2 × 2 × 2 Å domains). The thick lines refer to the calculated positions.

Comparison of the *t*-plots reveals cross-correlations between the strongest positional and ADP modulations. Minima of the ADP wave-like curves correspond to the extrema of the positional modulations, whereas the maxima of the ADP modulations correspond to inflection points of the curves of the positional modulation. Large departures of the atoms from their average positions may be assumed to require energy for straining the bond angles (although much less than changing the length of the strong Si—O bonds). It appears that increased strain corresponds to a reduced distribution of positions of the atoms (as described by small ADPs) owing to reduced thermal vibrations or static displacements. The inflection points of the positional modulations indicate locations where the atoms are close to their average positions, the strain of the bonding angles is relatively small and where the Debye–Waller parameters adopt large values. These findings mirror those of Jobst & van Smaalen (2002) for the occupational modulation in $(LaS)_{1.12}NbS_2$ where 'a tighter environment corresponds to smaller temperature factors, but larger values for the occupancy'.

For the O atoms that suffer the largest displacements, the overall shape of the modulation function of the average Debye–Waller factors (U_{eq}) resembles the variation of the intertetrahedral Si—O—Si angles (Fig. 7) although the Si—O—Si *t*-plots show larger deviations from a simple sinusoidal shape, which probably can be ascribed to additional contributions from the Si atoms. In silicate structures, the Si—O—Si angles can vary in the range from 120 to 180°. For silica polymorphs, a Si—

Table 3
Modulations of incommensurate high and low tridymite.

	L3-T_O(MX-1)	H3-T_O(OS)
Temperature range (K)	Below 338	~ 473–423
Average structure	*Cc*	$C112_1$†
Wavevector	($\alpha 0 \gamma$)	($\alpha \beta 0$)
Wavelength (Å)	~ 24	~ 65–100
Temperature dependence of the wavelength	Low	Large
Maximum amplitude (Å)	~ 0.6	~ 0.4‡

† In comparable pseudo-orthorhombic setting. ‡ At 438 K (Graetsch & Brunelli, 2005).

O—Si angle of ~ 147° (corresponding to a Si—Si distance of *ca* 3.06 Å) is considered to be strain-free. Less energy is necessary to widen an unstrained Si—O—Si bond angle than to narrow it (Liebau, 1985). The latter is made difficult mainly by cation–cation repulsions and by O–O repulsions of O atoms belonging to neighbouring tetrahedra. Minima of the ADP modulation correlate with minima of the Si—O—Si modulation, again indicating that the minima of the Debye–Waller factor modulation correspond to the strain maxima.

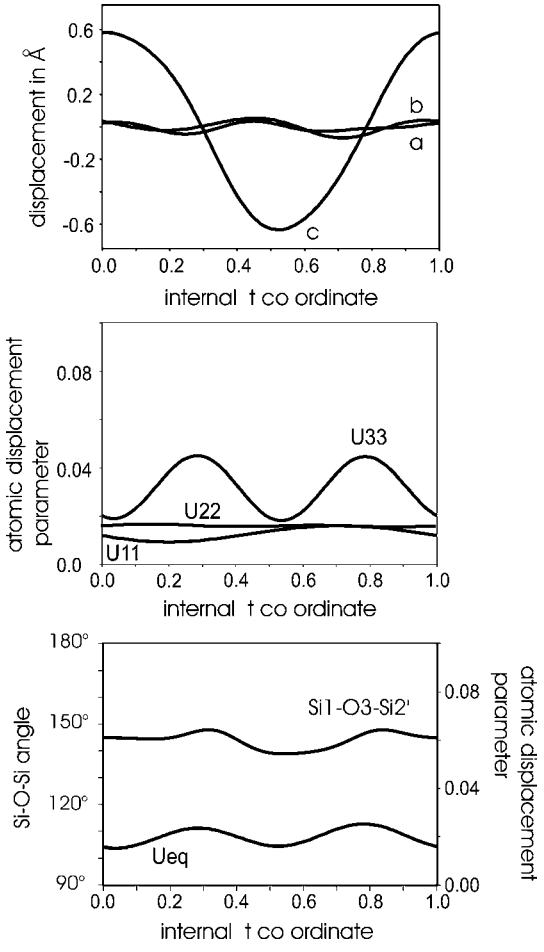

Figure 7
Variations of the isotropic (U_{eq}) and anisotropic ADPs (U^{11}, U^{22} and U^{33}) and the positional modulation of O3 along the internal *t* coordinate in comparison to the modulation of the Si1—O3—Si2 angle.

5. Conclusions

For silica tridymite, two different incommensurate displacive modulations exist in two different temperature ranges (Table 1). Although incommensurate low tridymite [L3-T_O(MX-1)] can be obtained by quenching high-temperature incommensurate tridymite [H3-T_O (OS)], the modulations of the two phases differ widely (Table 3), barely showing any relationship.

The refinement of the single-crystal diffraction data including third-order satellites reveals deviations from a simple harmonic shape of the modulation functions of incommensurate low tridymite, as was previously shown from powder data. The ADPs are also modulated. The ADP modulations correlate with the positional modulations.

The different configurations of the tetrahedra (*cis* and *trans*) in tridymite are suspected to cause the long sequence of phase transitions by preventing a cooperative collapse of the framework in a single step, as in cristobalite which exclusively contains *trans* configurations. Different displacement patterns of the modulations shed further light on the differences between *cis* and *trans* configurations of tetrahedra.

I would like to thank Professor Dr O. W. Flörke, Bochum, for the tridymite crystals, two anonymous reviewers for their valuable comments and Professor Dr V. Petříček for adding to the *JANA*2006 program suite the possibility of representing the modulation of the displacement parameters on the principal axes of the ellipsoids.

References

Baur, W. H. (1977). *Acta Cryst.* B**33**, 2615–2619.
Brandenburg, K. & Putz, H. (2005). *DIAMOND*, Version 3. Crystal Impact GbR, Postfach 1251, D-53002 Bonn, Germany.
Cellai, D., Carpenter, M. A., Wruck, B. & Salje, E. K. H. (1994). *Am. Mineral.* **79**, 606–614.
DeDombal, R. F. & Carpenter, M. A. (1993). *Eur. J. Mineral.* **5**, 507–622.
Dollase, W. A. (1967). *Acta Cryst.* **23**, 617–623.
Dollase, W. A. & Baur, W. H. (1976). *Am. Mineral.* **61**, 971–976.
Flörke, O. W. (1967). *Fortschr. Mineral.* **44**, 181–230.
Flörke, O. W. & Langer, K. (1972). *Contrib. Mineral. Petrol.* **26**, 221–230.
Flörke, O. W. & Nukui, A. (1988). *Neues Jahrb. Miner. Abh.* **158**, 175–182.
Gibbs, R. E. (1927). *Proc. R. Soc. London A*, **113**, 351–368.
Graetsch, H. A. (2001). *Phys. Chem. Miner.* **28**, 313–321.
Graetsch, H. A. (2003). *Z. Kristallogr.* **218**, 531–535.
Graetsch, H. A. & Brunelli, M. (2005). *Z. Kristallogr.* **220**, 606–613.
Graetsch, H. & Topalović-Dierdorf, I. (1996). *Eur. J. Mineral.* **8**, 103–113.
Hoffmann, W., Kockmeyer, M., Löns, J. & Vach, Chr. (1983). *Fortschr. Mineral.* **61**, 96–98.
Jobst, A. & van Smaalen, S. (2002). *Acta Cryst.* B**58**, 179–190.
Kato, K. & Nukui, A. (1976). *Acta Cryst.* B**32**, 2486–2491.
Kato, K., Nukui, A., Jarchow, O. & Löns, J. (1998). *Z. Kristallogr.* **213**, 392–398.
Kihara, K. (1977). *Z. Kristallogr.* **146**, 185–203.
Kihara, K., Matsumoto, T. & Inamure, M. (1986). *Z. Kristallogr.* **177**, 27–38.
Konnert, J. H. & Appleman, D. E. (1978). *Acta Cryst.* B**34**, 391–403.

Liebau, F. (1985). *Structural Chemistry of Silicates*. Berlin, Heidelberg: Springer-Verlag.
Löns, J. & Hoffmann, W. (1987). *Z. Kristallogr.* **178**, 141–143.
Nukui, A. & Nakazawa, H. (1980). *J. Mineral. Soc. Jpn*, **14**, 241–244.
Nukui, A., Nakazawa, H. & Akao, M. (1978). *Am. Mineral.* **63**, 1252–1259.
Nukui, A., Yamamoto, A. & Nakazawa, H. (1979). *Am. Inst. Phys. Conf. Proc.* No. 53, 327–329.
Oxford Diffraction (2006*a*). *CrysAlis CCD*. Oxford Diffraction.
Oxford Diffraction (2006*b*). *CrysAlisRED*, Version 171.31.5. Oxford Diffraction.
Petříček, V., Dušek, M. & Palatinus, L. (2006). *JANA*2006. Institute of Physics, Praha, Czech Republic.
Pryde, A. K. A. & Dove, M. T. (1998). *Phys. Chem. Miner.* **26**, 171–179.
Sato, M. (1964). *Mineral. J.* **4**, 215–225.
Schönleber, A., Meyer, M. & Chapuis, G. (2001). *J. Appl. Cryst.* **34**, 777–779.
Withers, R. L., Norén, L. & Liu, Y. (2004). *Z. Kristallogr.* **219**, 701–710.